Global NEST Journal, Vol 20, No X, pp XX-XX

Performance of granular activated carbon/nanoscale zero-valent iron for removal of humic substances from aqueous solution based on Experimental Design and Response Surface Modeling

Ahmadreza Yazdanbakhsh[1], Yalda Hashempour[2,3,*] and Mansour G. Haderpouri[4]
[1]Department of Environmental Health Engineering, School of Public Health, Shahid Beheshti University of Medical Sciences, Tehran, Iran.
[2]Department of Environmental Health Engineering, School of Public Health, Students' research committee, Shahid Beheshti University of Medical Sciences, Tehran, Iran.
[3]The Applied Science Center of Iran, University of Applied Science, Tehran, Iran.
[4]Department of Environmental Health Engineering, faculty of Health and nutrition, Lorestan University of Medical Sciences, Khoramabad, Iran.
Received: 13/02/2017, Accepted: 18/10/2017, Available online: 11/12/2017
*to whom all correspondence should be addressed: e-mail: yalda.hashempour@yahoo.com

Graphic Abstract

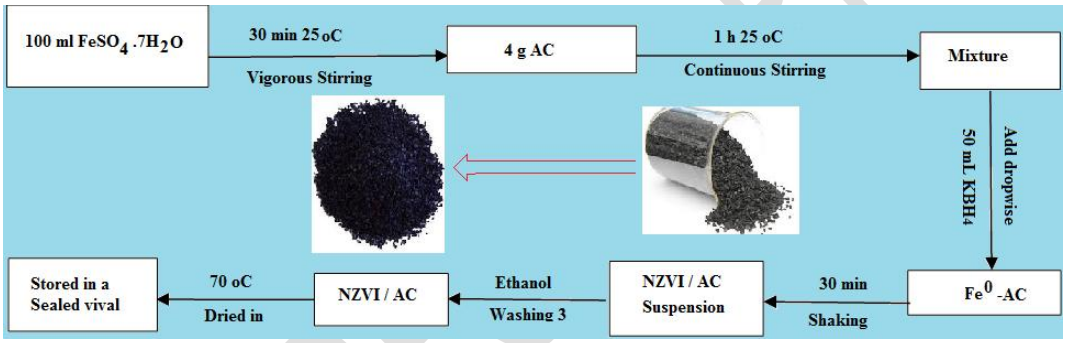

Abstract

Response surface methodology has been used to design experiments and to optimize the effect of independent variables responsible for higher adsorption of humic substances by activated carbon supported nanoscale zero-valent iron from aqueous solutions. The variables of initial concentration, time, pH, adsorbent dose was examined. The characterization of NZVI/AC was carried out by SEM-EDS and XRD analysis. The adsorption isotherms and kinetics of humic substances on AC and NZVI/AC were studied. The findings showed that the particle size of synthesis NZVI were in the range 20-50nm. The experimental data followed the Langmuir isotherm and pseudo-second kinetic model. For AC, optimum conditions of initial concentration, pH, contact time, and adsorbent dose were 5 mg L^{-1}, 4.43, 46.28 min, and 1.5 g L^{-1}, respectively. For NZVI/AC, optimum conditions of initial concentration, pH, contact time, and adsorbent dose were 5.48 mg L^{-1}, 5.44, 44.7 min, 0.65 g L^{-1}, respectively. Predicted removal efficiency by Box-Benken models for activated carbon and NZVI were 60 and 100 percent, respectively.

Keywords: adsorption, Humic Substances, activated carbon, NZVI/AC, design of experiments

1. Introduction

Water must be disinfected to provide clean and safe drinking water. The disinfection can be used in various combinations, such as chlorine, chloramine, Ozone, ClO_2. Of these compounds, chlorine compounds are used significantly throughout the world. Recently, due to existence organic material in the water, concerns about the by-product of the disinfection such as humic acid and acetic acid significantly increased. The primary source of formation of by-product disinfection, organic compounds are in the water resources(Golfinopoulos and Nikolaou, 2005). Humic substances are the most critical part of organic compounds. 60 to 90 percent of natural organic matter (NOM) is humic substances (Mansoori *et al.*, 2014). So far, various processes have been used to remove of humic substances such as UV-H_2O_2 (Bazri *et al.*, 2012), Fenton process (Wu *et al.*, 2011), ozonation (Yavich *et al.*, 2004), ion exchange and PAC (Humbert *et al.*, 2008), coagulation (Matilainen *et al.*, 2010), membrane filtration (Cui and Choo, 2014), adsorption–photodegradation (Wang *et al.*, 2013). Of these processes, adsorption

processes are more preferable. Because of lower cost, more straightforward operation. So far, various adsorbents for the removal of humic acid have been used such as chitosan (Chang and Juang, 2004), acicular goethite nanoparticles(Moreira *et al.*, 2017), natural zeolite (Moussavi *et al.*, 2011) Surfactant modified zeolite (Moreira *et al.*, 2017), polyaniline/attapulgite composite (Wang *et al.*, 2011), orange peel (Gupta and Nayak, 2012), poly ferric chloride (Zhan *et al.*, 2010), granular ferric hydroxide (GFH) (Genz *et al.*, 2008), bentonite (Doulia *et al.*, 2009). Recently, the use of metals with zero capacity (such as Al, Sn, Zn and Fe) to remove environmental pollutants is too considered. For these reasons, zero-valent iron (Fe°) has been more attention: abundance, inexpensive, non-toxic, fast reaction, high efficiency in removing contaminants from water (Fu *et al.*, 2015). Zero-valent iron is used very widely to remove various compounds such as chromium (VI) and lead (II) (Fu *et al.*, 2015, Sheng *et al.*, 2016, Qian *et al.*, 2017), phosphorus (Eljamal *et al.*, 2016), nitrobenzene (Li *et al.*, 2016), trichlorophenol (Chang *et al.*, 2015), heavy metals (Li *et al.*, 2017), phenol (Diao *et al.*, 2016), norfloxacin (Zhang *et al.*, 2017), nitrate and phosphate (Khalil *et al.*, 2017).

The purpose of this study was to investigate the use of activated carbon supported nanoscale zero-valent iron (NZVI/AC) as a new adsorbent for the removal of humic substances (HS) from water resources. The experimental work includes the assessment of factors influencing the HS adsorption on NZVI/AC using of an experimental design, Box–Behnken factorial design (BBD), in response surface methodology (RSM). The isotherm and kinetics models of HS on AC and NZVI/AC under various conditions were also studied.

2. Materials and methods

2.1 Chemicals and water sample

Commercial AC used in this study was Merck product. For synthesizing NZVI/AC adsorbent the following chemicals were needed: Iron (II) Sulfate Heptahydrate ($FeSO_4.7H_2O$), potassium borohydride, polyethylene glycol (PEG) and ethanol (99.7%, v/v). A stock solution of humic acid of 1,000 mg L^{-1} was prepared according to previous works (APHA, 2005). Stock solution stored in a refrigerator at 4±0.1 °C before use. All working solutions were prepared by diluting the stock solution ($C_1V_1=C_2V_2$).

2.2. Preparation of NZVI/AC

The commercial AC was soaked in 5% hydrochloric acid for 24 h, followed by washing with deionized water until the water pH was stable (pH=6.52–6.70). After drying for 24 h at 105 °C, AC was used as a supporter for NZVI particle. NZVI can be synthesized according to the previous study (Jianan Xiao *et al.*, 2014) by the following reaction:

$$Fe^{+2} + 2BH_4^- + 6H_2O \rightarrow Fe^0 \downarrow + 2B(OH)_3 + 7H_2 \uparrow \quad (1)$$

The procedure was described as follows: 1) 0.07 M of an iron solution was prepared by dissolving $FeSO_4.7H_2O$ in 100 mL of ethanol-water (ethanol/water = 3/7, v/v) with an addition of 0.5 g of PEG as a surfactant. 2) 50 mL of KBH4 reductant was added dropwise (2 mL/min) to a solution containing AC (4 g) and $FeSO_4.7H_2O$ under vigorous magnetic stirring. 3) after addition of KBH_4, the solution was shaken for another 30 min (Jianan Xiao *et al.*, 2014). 4) The NZVI/AC formed was filtered and alternately rinsed with ethanol and degassed RO water three times (Jianan Xiao *et al.*, 2014).

2.3 Characterization of NZVI/AC

The morphological properties of NZVI/AC adsorbent were observed with a scanning electron microscope (SEM, TESCAN Vega Model). Localized NZVI/AC analyses from chosen regions were obtained with an INCA electron dispersion spectrometer (EDS) in conjunction with SEM. The crystal structure and crystallinity of the composites were examined by XRD analysis using a Rigaku D/MAXYA diffract meter with Ni-filtered Cu Ka radiation as an X-ray source.

2.4 Equilibrium time

The HA solution with a concentration of 25 mgL^{-1} was prepared. Then 1 g of each adsorbent (AC and NZVI/AC) was poured separately into the flask. The pH of the solution in each flask was adjusted between 6.5 and 7. The speed of 200 rpm was used for proper mixing. The sampling from each flask was conducted at specified intervals and then filtered through 0.45 µ filter. The residual concentration of HA was determined by measuring the absorbance at the maximum wavelength of 254 nm using a 1 cm quartz cell in a spectrophotometer (DR5000, UV-Vis spectrophotometer, HACH, USA). The results of this phase were examined by drawing a graph of concentration versus time. When the concentration changes over time reach to zero, it was recorded as the equilibrium.

2.5 Isotherm and kinetic studies

From the various isotherm equations that are used for analysis absorption data in aqueous environments, the Langmuir and Freundlich isotherms are more common(Massoudinejad *et al.*, 2016). The linear form of these isotherms is shown as equation [2] (Langmuir) and [3] (Freundlich):

$$\frac{C_e}{q_e} = \frac{1}{k_L q_m} + \frac{1}{q_m} C_e \quad (2)$$

$$\ln q_e = \ln k_F + \frac{1}{n} \ln C_e \quad (3)$$

Where, q_m (mg/g) is the maximum adsorption capacity, q_e (mg/g) is the amount of HA, C_e (mg/L) is the equilibrium concentration of HA, k_F and n are the Freundlich constants, and k_1 (L/mg) is the Langmuir constant. To extract the adsorption isotherms of each adsorbent, HA in the concentration of 25 mg/L, different dosage of adsorbent (between 0.1 to 2 g l^{-1}), and contact time based on equilibrium time for AC and NZVI/AC adsorbents were used. The results of each phase were recorded. For Langmuir model and Freundlich model, the plot of 1/ (X/m) versus 1/C and the linear plot $\ln q_e$ versus $\ln C_e$ were drawn,

respectively. The determination coefficient (R^2) is used to determine the goodness of fit of the isotherm models.

The pseudo-first-order and pseudo-second-order kinetics were used to describe the data. The pseudo-first-order (equation 4) and the pseudo-second-order (equation 5) provided as follows:

$$\ln(q_e - q_t) = \log(q_e) - \frac{k_1}{2.303}t \qquad 4$$

$$\frac{1}{q_t} = (\frac{1}{k_2 q_e^2}) + (\frac{1}{q_e})t \qquad 5$$

Where, q_e and q_t are the amount of adsorbed HA on adsorbents at time t and equilibrium time, respectively. k_1 and k_2 are constants of adsorption rate. The HA in the concentration of 25 mg L^{-1}, adsorbent doses of 1 g L^{-1}, and contact time (between 0 to 150 min) was used to extract the adsorption kinetics of each adsorbent. The results of each phase were recorded. For the pseudo-first-order model and the pseudo-second-order model, the plot of ln (q_e-q_t) versus t and the plot t/q_t versus t were drawn, respectively. The R^2 is used to determine the goodness of fit of the kinetic models.

2.6 Experimental design

The Box–Behnken factorial design was used to optimize the HA removal. This design consists of three levels (low, medium and high coded as _1, 0, and +1, respectively). The complete design included of 58 runs and these were performed in duplicate to optimize the levels of selected variables (HA initial concentration, pH, contact time, adsorbent dose, and the type of adsorbent. For statistical calculations, the five independent variables were designated as X_1, X_2, X_3, X_4 and X_5, respectively, and they were coded according to the following equation:

$$X_j = \frac{X_i - X_0}{\Delta X_i} \qquad 6$$

Where X_j is the coded value of an independent variable, X_i is the real value of an independent variable, X_0 is the real value of an independent variable at the center point, and Δx_i is the step change value (Doddapaneni KK *et al.*, 2007). The lowest and highest levels of the variables were HA concentration 5 and 50, pH 3 and 9, time 1 and 60 minutes, adsorbent dose 0.5 and 1.5 g/L, respectively, and the type of adsorbents was AC and NZVI/AC. The removal efficiency of HA was multiply regressed the different parameters by the least square methods as follows:

$$Y = \beta_0 + \sum \beta_i X_i + \sum \beta_{ii} X_i^2 + \sum \beta_{ij} X_i X_j \qquad 7$$

Where Y is the predicted response variable; β_0, β_i, β_{ii} and β_{ij} are constant regression coefficients of the model; X_i and X_j (i = 1, 3; j = 1, 3, i≠j) represent the independent variables in the form of coded values. The accuracy and fitness of the above model were evaluated by R^2 and F value. Table 1 gives the Box–Behnken design matrix along with experimental and predicted values for HA removal in coded terms. The predicted values for HA removal were obtained by applying quadratic model (Design Expert software, Trial version 7, Stat ease). The optimum values of the variables for HA removal were obtained by solving the regression equation, by analyzing the response surface contour plots and constraints for the variable factors using the same software. The goal fixed for the HA removal was maximum HA removal.

2.7. Adsorption of HA Experiments

The adsorption experiments were performed in batch mode in 250 ml beakers by mixing 100 ml of the desired HA solution. The mixture was shacked at 200 rpm for the desired time. The mixture was then being filtered through 0.45 µ and the residual HA in the supernatant solution was determined by measuring the absorbance at the maximum wavelength of 254 nm using a spectrophotometer (DR5000, UV-Vis spectrophotometer, HACH, USA).

3. Results and discussion

3.1. Characterization of adsorbents

Properties and morphology of AC and NZVI/AC adsorbents were determined with SEM and EDS analysis in the operating voltage 20 keV (Fig. 1a and 1b).

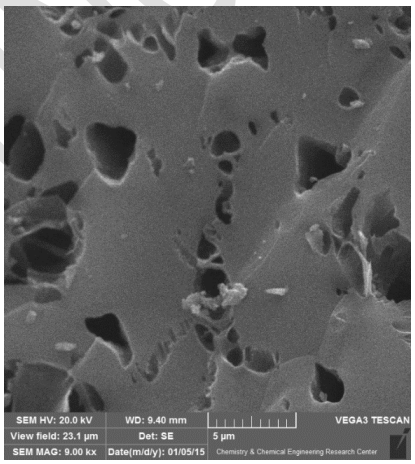

(a)

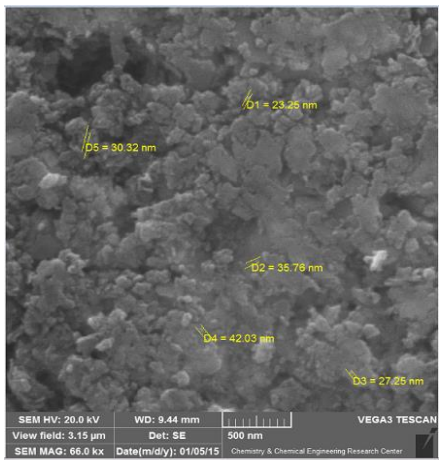

(b)

Figure 1. (a) SEM image of AC, (b) SEM image of NZVI/AC

Table 1. Box–Behnken design matrix in coded terms along with experimental and predicted values for HA removal.

Run	HA Concentration (mg L^{-1})	pH	Time (min)	Dose (gL^{-1})	Type	RE (%)	predicted
1	25	6	1	0.5	AC+NZVI	40.11	44.44
2	25	6	60	0.5	AC	46.56	54.32
3	50	6	60	1	AC	47.61	45.34
4	50	6	1	1	AC+NZVI	42.94	43.46
5	25	6	30	1	AC+NZVI	50.53	79.3
6	25	3	60	1	AC+NZVI	100	95.45
7	25	9	30	0.5	AC+NZVI	63.71	58.54
8	50	3	30	1	AC	53.65	54.46
9	5	3	30	1	AC+NZVI	100	99.21
10	25	3	30	1.5	AC+NZVI	97.92	100.05
11	25	6	30	1	AC+NZVI	80.76	79.3
12	5	6	30	1.5	AC+NZVI	95.48	94.69
13	50	6	30	0.5	AC	37.43	41.7
14	25	6	60	1.5	AC+NZVI	92.09	90.93
15	25	6	30	1	AC	50.53	50.93
16	50	9	30	1	AC+NZVI	34.11	57.56
17	25	6	30	1	AC	50.53	50.93
18	25	3	1	1	AC	31.08	36.83
19	25	9	30	1.5	AC+NZVI	79.93	74.78
20	5	6	60	1	AC+NZVI	93.27	90.09
21	25	6	30	1	AC+NZVI	80.76	79.3
22	25	9	1	1	AC+NZVI	41.59	39.93
23	5	3	30	1	AC	65.99	70.84
24	50	3	30	1	AC+NZVI	90.52	82.83
25	25	9	30	1.5	AC	32	38.42
26	25	6	30	1	AC	50.53	50.93
27	25	6	60	0.5	AC+NZVI	75.5	74.7
28	25	6	1	1.5	AC+NZVI	57.07	60.68
29	25	6	1	0.5	AC	10.99	24.07
30	25	6	1	1.5	AC	25.73	24.32
31	25	9	30	0.5	AC	63.71	38.17
32	5	9	30	1	AC	34.19	45.57
33	5	6	60	1	AC	60	61.73
34	50	9	30	1	AC	16.88	29.19
35	25	6	30	1	AC	50.53	50.93
36	25	3	30	1.5	AC	64.26	63.68
37	5	6	30	1.5	AC	63.23	58.33
38	50	6	30	0.5	AC+NZVI	65.72	62.08
39	25	3	30	0.5	AC	91.17	63.44
40	25	3	1	1	AC+NZVI	68.87	65.2
41	50	6	30	1	AC+NZVI	74.99	70.19
42	50	6	60	1.5	AC+NZVI	86.18	81.83
43	25	6	30	1	AC+NZVI	80.76	79.3
44	25	9	60	1	AC+NZVI	76.06	70.18
45	5	6	30	1	AC	56.96	58.21
46	25	6	30	1	AC+NZVI	80.76	79.3
47	25	9	1	1	AC	41.59	11.56
48	25	3	30	0.5	AC	51.35	63.44
49	5	6	1	1	AC	26.36	31.47
50	25	3	60	1	AC	60.57	67.08
51	25	6	30	1	AC+NZVI	80.76	79.3
52	50	6	1	1	AC	14.34	15.09
53	25	6	60	1.5	AC	60.76	54.57
54	25	9	60	1	AC	29.42	41.81
55	5	6	1	1	AC+NZVI	56.22	59.84
56	5	9	30	1	AC+NZVI	79.35	73.94
57	50	6	30	1.5	AC	51.35	41.95
58	5	6	30	0.5	AC+NZVI	78.89	78.46

X_1=HA concentration, X_2=pH, X_3= Time, X_4=adsorbent dose and X_5= Type of adsorbent

The image magnification electron is 9,000 times. These analyses show the quantitative characteristics, such as the particle size, shape/morphology and surface area of the adsorbents. Fig. 1a displays that the AC was some deal

spherical and these spherical particles have hole-like structures. This property increased the available and specific surfaces for more reaction. In Fig. 1b, we can see that the size of NZVI ranged from 20–50 nm. The NZVI particles were immobilized on the surface or inside the pores of AC. Apparently, the immobilization of NZVI using AC prevented their aggregation which was beneficial to maintaining their high surface area and reactivity (Jianan Xiao *et al.*, 2014).

The results of the analysis of SEM-EDS (Fig. 2a and 2b) show the elemental analysis of AC and NZVI/AC. As it can be seen in Fig. 2a, the two main elements in the AC were carbon and oxygen that it was included 90.39 and 9.61 % by weight, respectively. Fig. 2b demonstrated that NZVI particles were distributed on the surface or loaded into the pores of AC. The Fe loaded on AC randomly. Moreover, the presence of a Fe peak at 0.5 keV in the EDS spectrum could be formed of Fe_2O_3 or Fe_3O_4. The oxide may appear due to the oxidation of Fe during the transfer and processing of the material for characterization. But, the peak at 0.5 keV was weak, implying that most Fe element was present as Fe^0. Thus, it could also be deduced that NZVI particles were successfully loaded onto AC and had excellent properties compared with non-supported particles. In Fu *et al.* study, the size of NZVI was 20 -60 nm and nanoparticles of iron were in the form of spherical particles (Fu *et al.*, 2015). In Sheng *et al.* NZVI was spherical with particle sizes in a range of 10e100 nm and aggregated together to remain in thermodynamically stable. Also, the peak at 706.5 eV in the spectra showed the existence of zero-valent iron, whereas the broad peaks at 712.5 and 726.3 eV were attributed to iron oxides and hydroxides, respectively (Sheng *et al.*, 2016).

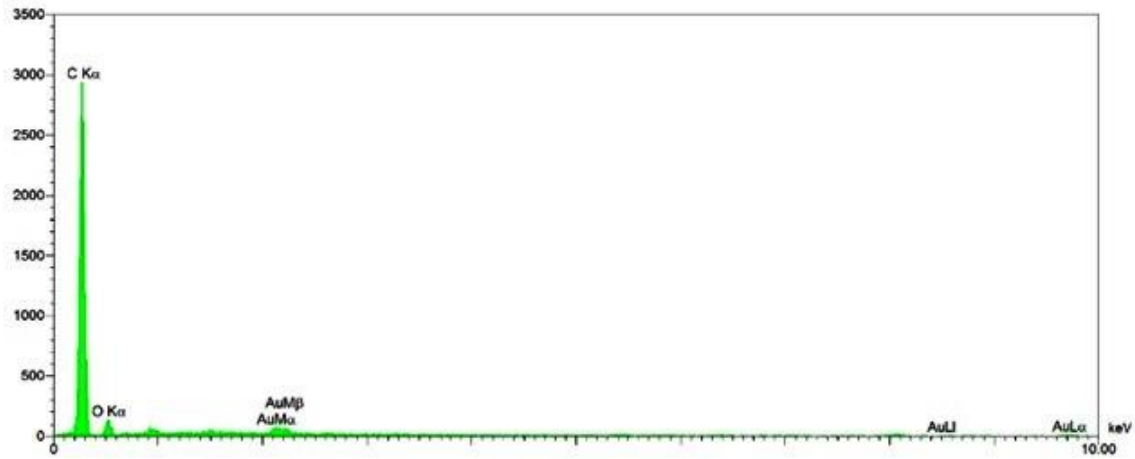

(a)

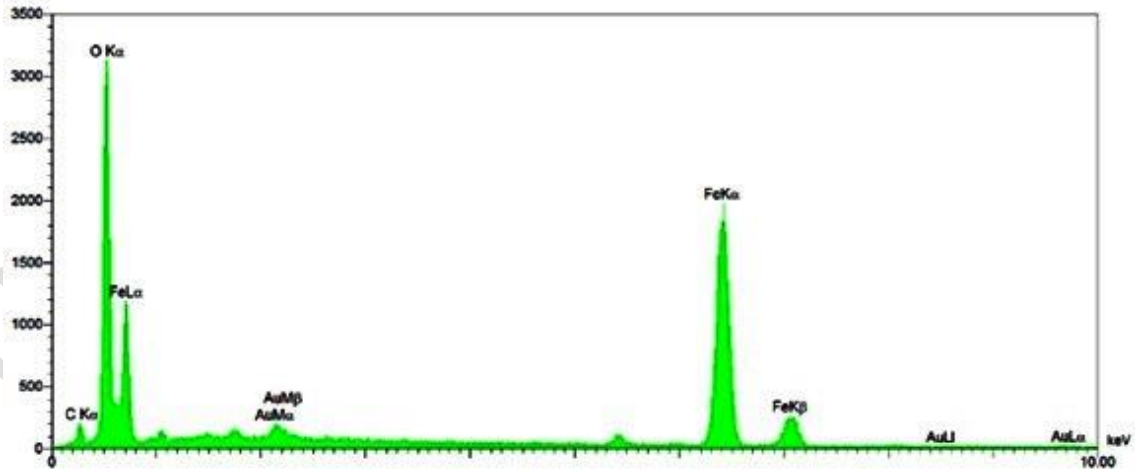

(b)

Figure 2. (a) EDS diagrams of AC, (b) EDS diagrams of NZVI/AC

The XRD diffraction patterns of AC and NZVI/AC are illustrated in Fig. 3a and 3b, respectively. In the pattern of AC, there was only one broad peak at 24.14 corresponding to amorphous carbon (Jianan Xiao *et al.*, 2014). The apparent peak at a 2h of 43.21 (Jianan Xiao *et al.*, 2014) in NZVI/AC indicates the presence of Fe^0. The wide-angle XRD suggests that the iron species are dispersed, forming tiny crystalline particles with sizes below the detection limit of X-ray diffraction. No characteristic diffraction peaks of

Fe_2O_3 and Fe_3O_4 were detected, suggesting that the iron was mainly in its Fe^0 state.

In the Eljamal *et al.* study, XRD spectra show that there was main peak intensity of NZVI at 44.8° indicating the presence of zero-valent iron in the synthesized nanoscale iron(Eljamal *et al.*, 2016). In Dong *et al.* study, the peaks 45 and 65 should be assigned to zero iron (Dong *et al.*, 2016).

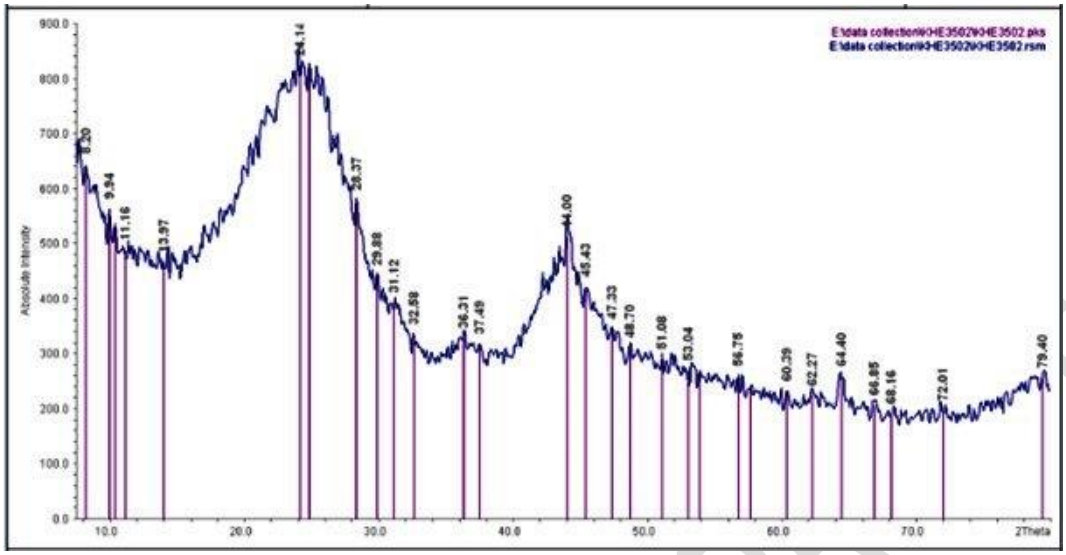

(a)

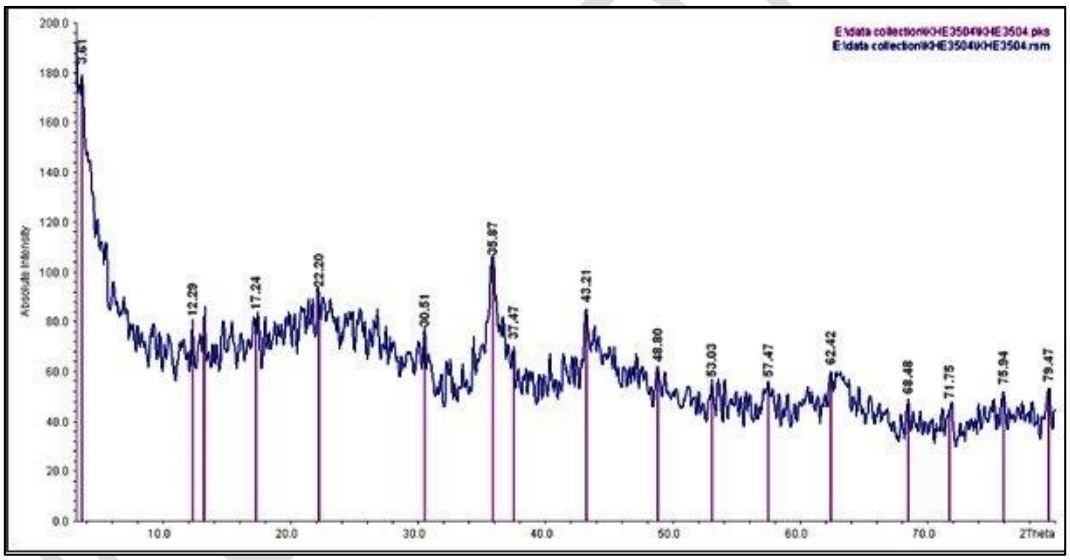

(b)

Figure 3. (a) XRD patterns of AC, (b) XRD patterns of NZVI/AC

3.2. Isotherm study

Getting the equilibrium time is the primary result of adsorption kinetics. If this parameter is specified, the adsorption isotherms can be achieved. The equilibrium time of HA for AC and NZVI/AC was 960 min and 360 min, respectively. Adsorption isotherms are equilibrium data that used to describe the interaction between adsorbent and adsorbate (MOHSENIBANDPEI *et al.*, 2016). Isotherms also suggest the maximum capacity of an adsorbent. The results of Langmuir and Freundlich isotherm models are shown in Fig. 4a and 4b, respectively and also in Table 2. As was clear from the results and determination coefficient, Langmuir model was able to better explain test results for AC (R^2=0.9911) and NZVI/AC (R^2=0.9939). An empirical equation of Langmuir isotherm is based on mono-layer, homogeneous adsorbed materials on the adsorbent. The results of Fu *et al.* study show that isotherm the removal of Cr on NZVI a better fit by Langmuir model (0.9989). The maximum capacity of NZVI to Cr was 36.1 mg g^{-1}. Also, the "n" factor was 2.4 (the normal range of n is between 1-10), which showed that the adsorption process could be considered to be favorable (Fu *et al.*, 2017). In Azari *et al.* study, the removal of nitrate on nZVI were consistent with Langmuir model. The coefficient of determination for Langmuir and Freundlich were 0.997 and 0.823, respectively (Azari *et al.*, 2014).

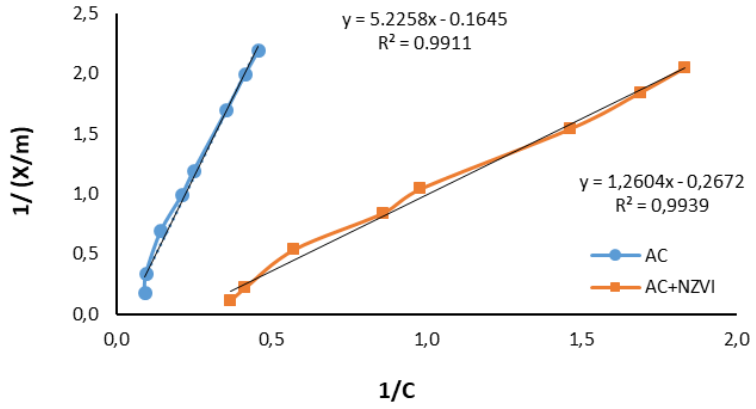

(a)

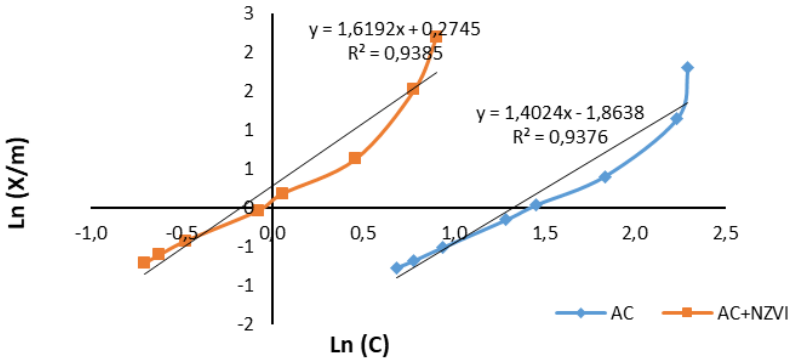

(b)

Figure 4. (a) Langmuir model of HA adsorption on AC and NZVI/AC (concentration= 25 mg L^{-1}, pH=6-7.5, T=25 °C, mixing time for AC=16 h and, for NZVI/AC=6 h), (b) Freundlich model of HA adsorption on AC and NZVI/AC (concentration= 25 mg L^{-1}, pH=6-7.5, T=25°C, mixing time for AC=16 h and, for NZVI/AC=6 h)

Table 2. Isotherm constants of Langmuir and Freundlich in adsorption of HA

Adsorbent	Langmuir			Freundlich		
	b	q_m	R^2	k_F	n	R^2
AC	-6.0786	34.7	0.9903	0.1551	0.7131	0.9376
NZVI/AC	-3.7419	46.1	0.9938	1.3158	0.6176	0.9384

3.3. Kinetic study

It is necessary to study the kinetics of the process to investigate the factor influencing the reaction rate. Adsorption kinetics were considered to better understanding the adsorption dynamic of HA on the adsorbent and producing a predictive model to estimate an amount of ions absorbed during the process provides. Fig. 5a and 5b show pseudo-first-order and pseudo-second-order kinetics curves, respectively. R^2 obtained for the first pseudo-models for AC, and NZVI/AC were 0.5424 and 0.9164, respectively. R^2 obtained for the second pseudo-models were 0.9999 and 0.9996, respectively. Therefore, both models are fit for the data, but the pseudo-second kinetic model was more acceptable for analysis of HA on both adsorbents. The pseudo-first-order kinetic model is based on absorbent capacity and is applied when adsorption using diffusion mechanism occurs within a boundary layer while the pseudo-second-order kinetic model shows that chemical adsorption is dominant and controlling mechanism in the process of adsorption (**21**).

Kinetic study Fu *et al.* showed that the removal of Cr and Pb followed a pseudo-first-order model(Fu *et al.*, 2015). The findings of Eljamal *et al.* indicate the experimental data followed the pseudo-first-order kinetic model with a high coefficient of determination (R^2=0.99 at pH=7). Adsorption of PO_4^{-3} using nZVI in acidic conditions had the highest reaction rate (removal efficiency 99.4 % at pH=2 and k_1= 10.56 h^{-1} (Eljamal *et al.*, 2016). Dong et al carried out the kinetic study of Cr (VI) reduction in the absence and presence of FA using kinetic models (three types). The pseudo-second-order model provides a better fit with the experimental data (R^2 were ranged 0.82-0.89) than the others.

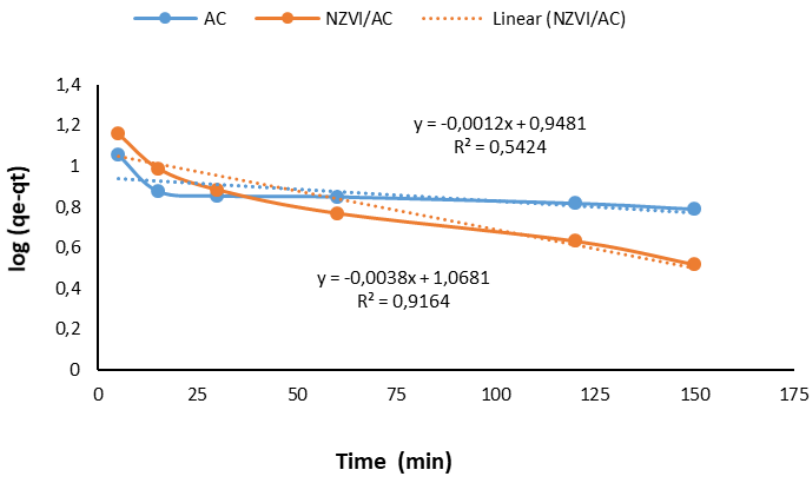

(a)

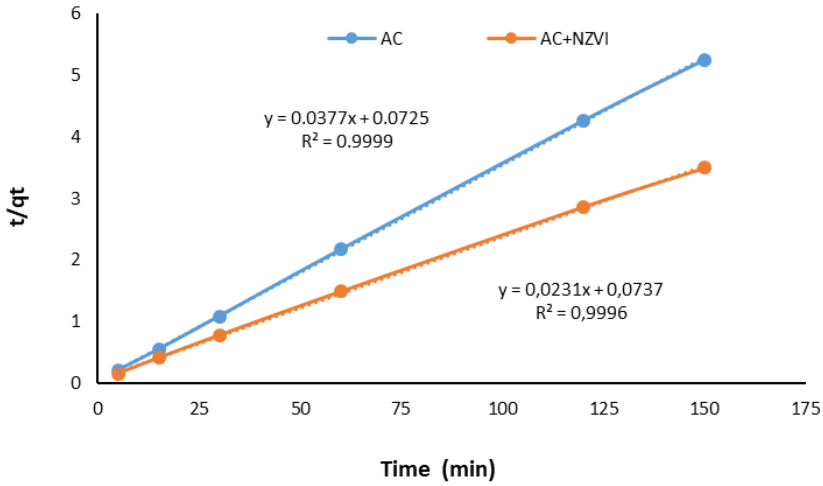

(b)

Figure 5. (a) First order reaction of HA adsorption on AC and NZVI/AC (concentration= 25 mg L^{-1}, pH=6-7.5, T=25 °C), Freundlich model of HA adsorption on AC and NZVI/AC (concentration= 25 mg L^{-1}, pH=6-7.5, T=25 °C)

3.4. Optimization of parameters for HA removal

Table 1 shows that there was a considerable variation in the HA removal by AC and NZVI/AC at different values of selected parameters. The data were analyzed by applying multiple regression analysis methods based on Equation 7. The predicted response Y for HA removal was obtained. Final equation regarding actual factors for AC and NZVI/AC were given as:

For AC

$$Y = 3.93 + 0.018X_1 + 0.21X_2 + 0.12X_3 + 0.94X_4 - 0.007X_1X_2 + 0.0001X_1X_3 + 0.005X_1X_4 - 0.004X_2X_3 - 0.21X_2X_4 - 0.007X_3X_4 - 0.0002X_1^2 + 0.0006X_2^2 - 0.001X_3^2 + 0.47X_4^2 \quad (8)$$

For NZVI/AC

$$Y = 5.87 + 0.019X_1 + 0.16X_2 + 0.12X_3 + 1.3X_4 - 0.007X_1X_2 + 0.0001X_1X_3 + 0.005X_1X_4 - 0.004X_2X_3 - 0.21X_2X_4 - 0.007X_3X_4 - 0.0002X_1^2 + 0.0006X_2^2 - 0.001X_3^2 + 0.47X_4^2 \quad (9)$$

In these equations, Y is the predicted response variable, i.e., the HA removal (%), X_1, X_2, X_3, and X_4 were HA concentration, pH, contact time, and adsorbent dose, respectively. The obtained data from Equation 8 and 9 were significant. It is verified by F value and the analysis of variance (ANOVA) by fitting the data of all independent

observations in the response surface quadratic model. Large the F value, the more significant is the corresponding term. According to the table 3, the model F-value of 16.08 with corresponding p<0.0001 implies the model was significant and can appropriately explain the relationship between response and independent variables. There was only a 0.01% chance that a model F-value this large could occur due to noise. The significance of each coefficient of Equation 8 and 9 was determined by applying t-test, and p-values of each are listed in Table 3. The p-values < 0.05 were considered as significant. Sum of the square (SS) should also be checked while considering the significance of a particular variable. The more value of SS increases the more significant of that variable increases. In this study, the high SS (26908.87) indicates that the model was significant. The lack of fit F-value of 0.90 implies the lack of fit is not significant relative to the pure error. There is a 61.25% chance that a lack of fit F-value this large could occur due to noise (Non-significant lack of fit is good). The effects of linear coefficients of HA concentration, pH, contact time, adsorbent dose, and the type of adsorbent was significant (P_{valve}<0.05). The interactive effects of the independent variables were insignificant (P_{valve}<0.05) The quadratic coefficients had negative effects. In the quadratic terms, contact time (X_3^2) is more significant (P_{valve}=0.0002) . Thus, statistical analysis of data shows that small variations in the values of the selected variables alter the HA removal efficiency. In this model X_1, X_2, X_3, X_4, and X_3^2 were significant model terms. Analysis of variance (ANOVA) for response surface quadratic model gave F-value 498.37, the R^2 value of 0.996, probability < 0.0001 and coefficient of variation (C.V. = 3.37%) signifying that model was highly significant and experiments were highly accurate and reliable (Table 3).

Table 3. Analysis of variance (ANOVA), regression coefficient estimate and test of significance for HA removal (response surface quadratic model).

Factor	Sum of squares	Mean squares	Coefficient estimated±S.E	d.f.	F-value	Probability (p) > F
Intercept (Model)	26908.87	1416.26	62.43±2.92	19	16.08	< 0.0001
X_1	1539.83	1539.83	-8.09±1.93	1	17.49	0.0002
X_2	3551.14	3551.14	-12.27±1.93	1	40.33	< 0.0001
X_3	5187.02	5187.02	15.03±1.96	1	58.91	< 0.0001
X_4	572.44	572.44	5.06±1.98	1	6.50	0.0149
X_5	12467.99	12467.99	14.82±1.25	1	141.60	< 0.0001
X_1X_2	267.61	267.61	-5.76±3.30	1	3.04	0.0894
X_1X_3	0.52	0.52	-0.26±3.41	1	0.01	0.9390
X_1X_4	1.12	1.12	0.42±3.71	1	0.01	0.9108
X_1X_5	20.32	20.32	-0.93±1.93	1	0.23	0.6337
X_2X_3	180.17	180.17	-4.75±3.32	1	2.05	0.1608
X_2X_4	154.44	154.44	-4.39±3.32	1	1.75	0.1933
X_2X_5	173.99	173.99	-2.69±1.92	1	1.98	0.1679
X_3X_4	0.46	0.46	0.23±3.23	1	0.01	0.9431
X_3X_5	108.90	108.90	2.15±1.93	1	1.24	0.2731
X_4X_5	109.22	109.22	2.23±2	1	1.24	0.2724
X_1^2	1.83	1.83	-0.392.68	1	0.02	0.8862
X_2^2	25.56	25.56	1.40±2.59	1	0.29	0.5931
X_3^2	1539.93	1539.93	-10.92±2.61	1	17.49	0.0002
X_4^2	53.05	53.05	2.05±2.65	1	0.60	0.4424
Residual	3345.92	88.05		38		
Lack of fit	2584.38	86.15		30	0.9	0.6125
Pure error	761.54	95.19		8		
Corrected total	146.69			57		

Experimental and predicted data for HA removal lie within a narrow interval (table 1). This also shows the excellent degree of fitness for the model equation. The main objective of the optimization was to determine the optimum values of variables for removal efficiency of HA. In optimization, the desired aim regarding removal efficiency was defined as a target to achieve maximum removal efficiency. For AC at an optimum concentration (5 mg /l), pH (4.43), contact time (46.28 min), and dose (1.5 g L^{-1}) the model predicted 60% removal efficiency. But for NZVI/AC at optimum concentration (5.48 mg L^{-1}), pH (5.44), contact time (44.7 min), and dose (0.65g L^{-1}) the model predicted 100% removal efficiency.

3.5. The effect of HA concentration and pH

Response surface contour plots help to understand the relationship between the response and experimental levels of each variable. These plots also show the type of interaction between test variables and help to obtain the optimum conditions (Myers RH and DC., 1995). Fig. 7 shows HA removal as a result of interaction between concentration and pH. The initial concentration was 5, 25, and 50 mg L^{-1}. The points on the corners and center of the figure represent experimental design points. The point with number 6 in the center indicates that contour plots have been drawn when the value of the fixed variable is at

the midpoint of lowest and highest selected levels. Colors for the contour plots represent the removal efficiency. For example, red means the maximum removal, green medium and blue minimum remove efficiency. For both adsorbents, as HA concentration increased the removal efficiency decreased. The results show that with an increase in concentration, these organic contaminant molecules can be adsorbed on the surface of adsorbents and these ions can be occupied a more significant number of active sites on the particle surface (Babuponnusami A and Muthukumar K, 2012). Thus, at a lower concentration, a large number of pores on the sorbent surface was available for reaction. Generally, the initial concentration of pollutants is a significant factor for the productivity of the adsorbent. As results demonstrated, acidic conditions were more suitable for the removal of HA. So that the highest removal efficiency was observed at acidic pH for both absorbent and when pH was greater than 6, the removal efficiency was decreased. At acidic pH, the concentration of H^+ ions increases and the surface of adsorbent has a positive charge by adsorption of the protons. On the other hand, HA is an anionic compound, and most of this contaminants were efficiently reduced at lower pH values (Zhang WH *et al.*, 2007). In this situation, HA is negatively charged, so the electrostatic attraction between the adsorbent and contaminants is the main cause of increased efficiency in the acid condition. At alkaline conditions, the hydroxide functional groups increase leading to a negative electric charge in the absorbent surface. Thus, the weak interaction or even repulsive force between the contaminant and the adsorbent will be created, which reduces the removal efficiency. As shown in Fig. 6, the maximum removal efficiency occurred at a concentration of about 5 mg/L and pH nearly 3. The removal efficiency was 53.68% and 97.23% for AC and NZVI/AC, respectively.

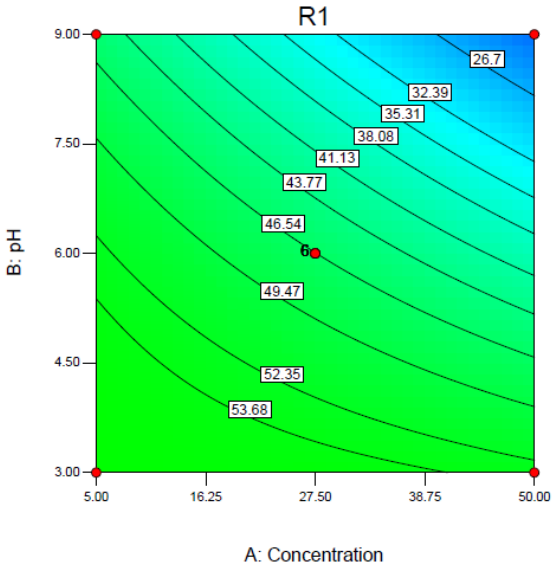

(a)

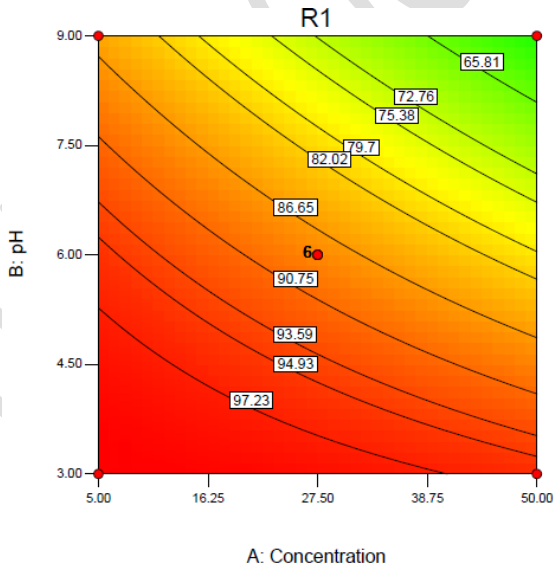

(b)

Figure 6. (a) Response surface contour plots showing the effect of concentration (mg/L) and pH on HA removal (%) by AC, (b) Response surface contour plots showing the effect of concentration (mg/L) and pH on 4HA removal (%) by NZVI/AC.

3.6. The effect of contact time and AC dosage

As it can be seen in Fig. 7a and 7b, by increasing the contact time from 1 to 60 min, the removal efficiency was increased in all doses. But by increasing the contact time from 30 to 60 min efficiency was increased in the form of a minor because the plot slope was reduced. This shows that in the first stages of adsorption, a large number of binding sites available for adsorption of HA. But over time due to the accumulation of pollutants on the surface of adsorbent and repulsive forces between adsorbed molecules on a solid surface and molecules in solution phase, the rate of adsorption is reduced. As a result of this incident, the adsorbent is saturated and cannot absorb more pollutants. Therefore, to create economic conditions and achieve a reduction in energy consumption, contact time of 30 minutes was selected as the optimum time (Tsenga *et al.*, 2011, Cheng *et al.*, 2005).

4. Conclusion

To conclude, granular activated carbon coated with nano zero-valent iron appears effective in removal of humic substances. The coupling of AC with NZVI induced a synergistic process which allowed for a maximum removal of humic substances thus providing the feasibility of this adsorbent. Moreover, based on Experimental Design and Response Surface Modeling using Box-Behnken factorial design, The effects of linear coefficients of HA concentration, pH, contact time, adsorbent dose, and the type of adsorbent was significant (P-value<0.05). The interactive effects of the independent variables were insignificant (P-value<0.05). The quadratic coefficients had negative effects. In the quadratic terms, contact time (X_3^2) is more significant (P-value=0.0002). Thus, statistical analysis of data shows that small variations in the values of the selected variables alter the HA removal efficiency. Analysis of variance (ANOVA) for response surface quadratic

model shows that the experiments are highly accurate and the model is highly significant, and experiments were highly accurate and reliable. Also, this shows the excellent degree of fitness for the model equation.

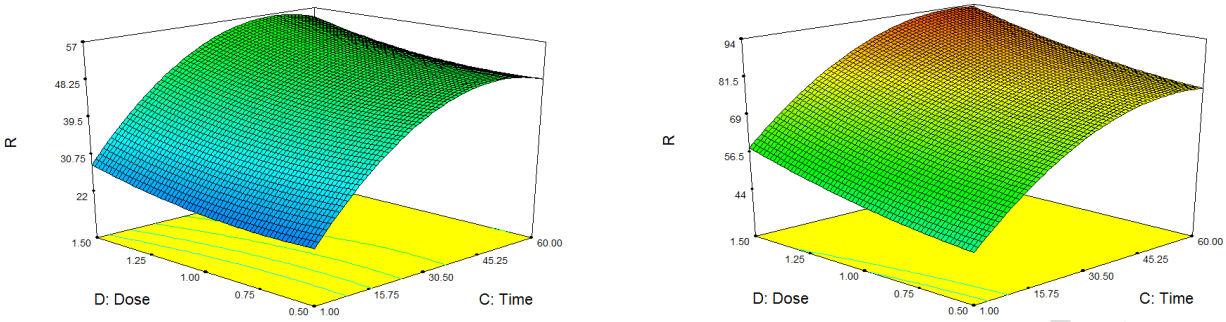

(a) (b)

Figure 7. (a) Response surface 3D plots showing the effect of contact time (minute) and dose (g/L) on HA removal (%) by AC, (b) Response surface 3D plots showing the effect of contact time (minute) and dose (g/L) on HA removal (%) by NZVI/AC.

Acknowledgement

The authors are most grateful to the laboratory staff of the Department of Environmental Health Engineering, School of Public Health, Shahid Beheshti University of Medical Sciences, for the financial support and their collaboration in this research.

References

APHA A.A.W. (2005). *Standard Methods for the Examination of Water and Wastewater,* 21th ed, American Health Public Association, Washington DC.

Azari A., Babaie A.-A., Rezaei-Kalantary R., Esrafili A., Moazzen M. and Kakavandi B. (2014), Nitrate removal from aqueous solution by carbon nanotubes magnetized with nano zero-valent iron, *Journal of Mazandaran University of Medical Sciences,* **23,** 15-27.

Babuponnusami A. and Muthukumar K. (2012), Removal of phenol by heterogenous photo electro Fenton-like process using nano-zero valent iron, *Sep Purif Tech,* **98,** 130-135.

Bazri M.M., Barbeau B. and Mohseni M. (2012), Impact of UV/H 2 O 2 advanced oxidation treatment on molecular weight distribution of NOM and biostability of water, *Water Research,* **46,** 5297-5304.

Chang J., Woo H., Ko M.-S., Lee J., Lee S., Yun S.-T. and Lee S. (2015), Targeted removal of trichlorophenol in water by oleic acid-coated nanoscale palladium/zero-valent iron alginate beads, *Journal of Hazardous Materials,* **293**, 30-36.

Chang M.-Y. and Juang R.-S. (2004), Adsorption of tannic acid, humic acid, and dyes from water using the composite of chitosan and activated clay, *Journal of Colloid and Interface Science,* **278**, 18-25.

Cheng W., Dastgheib S.A. and Karanfil T. (2005), Adsorption of dissolved natural organic matter by modified activated carbons, *Water Research,* **39**, 2281-2290.

Cui X. and Choo K.-H. (2014), Natural organic matter removal and fouling control in low-pressure membrane filtration for water treatment, *Environmental Engineering Research,* **19**, 1-8.

Diao Z-H., Xu X-R., Chen H., Jiang D., Yang Y-X., Kong L-J., Sun Y-X., Hu Y-X., Hao Q-W. and Liu L. (2016), Simultaneous removal of Cr (VI) and phenol by persulfate activated with bentonite-supported nanoscale zero-valent iron: Reactivity and mechanism, *Journal of hazardous materials,* **316,** 186-193.

Doddapaneni K.K., Tatineni R., Potumarthi R. and Ln M. (2007), Optimization of media constituents through response surface methodology for improved production of alkaline proteases by Serratia rubidaea, *J Chem Technol Biotechnol,* **82,** 721–729.

Dong H., Ahmad K., Zeng G., Li Z., Chen G., He Q., Xie Y., Wu Y., Zhao F. and Zeng Y. (2016), Influence of fulvic acid on the colloidal stability and reactivity of nanoscale zero-valent iron, *Environmental Pollution,* **211**, 363-369.

Doulia D., Leodopoulos C., Gimouhopoulos K. and Rigas F. (2009), Adsorption of humic acid on acid-activated Greek bentonite, *Journal of Colloid and Interface Science,* **340**, 131-141.

Eljamal O., Khalil A.M., Sugihara Y. and Matsunaga N. (2016), Phosphorus removal from aqueous solution by nanoscale zero valent iron in the presence of copper chloride, *Chemical Engineering Journal,* **293**, 225-231.

Fu R., Yang Y., Xu Z., Zhang X., Guo X. and Bi D. (2015), The removal of chromium (VI) and lead (II) from groundwater using sepiolite-supported nanoscale zero-valent iron (S-NZVI), *Chemosphere,* **138**, 726-734.

Fu R., Zhang X., Xu Z., Guo X., Bi D. and Zhang W. (2017), Fast and highly efficient removal of chromium (VI) using humus-supported nanoscale zero-valent iron: Influencing factors, kinetics and mechanism, *Separation and Purification Technology,* **174**, 362-371.

Genz A., Baumgarten B., Goernitz M. and Jekel M. (2008), NOM removal by adsorption onto granular ferric hydroxide: Equilibrium, kinetics, filter and regeneration studies, *Water research,* **42**, 238-248.

Golfinopoulos S.K. and Nikolaou A.D. (2005), Survey of disinfection by-products in drinking water in Athens, Greece, *Desalination,* **176**, 13-24.

Gupta V. and Nayak A. (2012), Cadmium removal and recovery from aqueous solutions by novel adsorbents prepared from orange peel and Fe_2O_3 nanoparticles, *Chemical Engineering Journal,* **180**, 81-90.

Humbert H., Gallard H., Suty H. and Croué J.-P. (2008), Natural organic matter (NOM) and pesticides removal using a combination of ion exchange resin and powdered activated carbon (PAC), *Water Research,* **42**, 1635-1643.

Jianan Xiao, Qinyan Yue, Baoyu Gao, Yuanyuan Sun, Jiaojiao Kong, Yuan Gao, Qian Li and Wang Y. (2014), Performance of

activated carbon/nanoscale zero-valent iron for removal of trihalomethanes (THMs) at infinitesimal concentration in drinking water, *Chemical Engineering Journal,* **253**, 63–72.

Khalil A.M., Eljamal O., Amen T.W., Sugihara Y. and Matsunaga N. (2017), Optimized nano-scale zero-valent iron supported on treated activated carbon for enhanced nitrate and phosphate removal from water, *Chemical Engineering Journal,* **309**, 349-365.

Li S., Wang W., Liang F. and Zhang W.-X. (2017), Heavy metal removal using nanoscale zero-valent iron (nZVI): theory and application, *Journal of Hazardous Materials,* **322**, 163-171.

Li X., Zhao Y., Xi B., Mao X., Gong B., Li R., Peng X. and Liu H. (2016), Removal of nitrobenzene by immobilized nanoscale zero-valent iron: Effect of clay support and efficiency optimization, *Applied Surface Science,* **370**, 260-269.

Mansoori F., Kalankesh L.R. and Malakootian M. (2014), Kinetics and Isothermic Behavior of SiO_2 Nanoparticles in Removal of Humic Acid from Aqueous Solutions: a case study on the Alavian Dam in Maragheh City, Iran, *Journal of Health and Development,* **3**, 71-83.

Massoudinejad M., Ghaderpoori M., Shahsavani A. and Amini M.M. (2016), Adsorption of fluoride over a metal organic framework Uio-66 functionalized with amine groups and optimization with response surface methodology, *Journal of Molecular Liquids,* **221**, 279-286.

Matilainen A., Vepsäläinen M. and Sillanpää M. (2010), Natural organic matter removal by coagulation during drinking water treatment: a review, *Advances in colloid and interface science,* **159**, 189-197.

Mohsenibandpei A., Alinejad A., Bahrami H. and Ghaderpoori M. (2016), Water solution polishing of nitrate using potassium permanganate modified zeolite: Parametric experiments, kinetics and equilibrium analysis, *Global NEST Journal*, **18**(3), 546-558.

Moreira R.F.P.M., Vandresen S., Luiz D.B., José H.J. and Puma G.L. (2017), Adsorption of arsenate, phosphate and humic acids onto acicular goethite nanoparticles recovered from acid mine drainage, *Journal of Environmental Chemical Engineering,* **5**, 652-659.

Moussavi G., Talebi S., Farrokhi M. and Sabouti R.M. (2011), The investigation of mechanism, kinetic and isotherm of ammonia and humic acid co-adsorption onto natural zeolite, *Chemical Engineering Journal,* **171**, 1159-1169.

Myers Rh and Dc. M. (1995), *Surface Methodology: Process and Product Optimization Using Designed Experiments,* 1st ed, Wiley-Interscience, New York.

Qian L., Zhang W., Yan J., Han L., Chen Y., Ouyang D. and Chen M. (2017), Nanoscale zero-valent iron supported by biochars produced at different temperatures: Synthesis mechanism and effect on Cr(VI) removal, *Environmental Pollution,* **223***,* 153-160.

Sheng G., Hu J., Li H., Li J. and Huang Y. (2016), Enhanced sequestration of Cr (VI) by nanoscale zero-valent iron supported on layered double hydroxide by batch and XAFS study, *Chemosphere,* **148**, 227-232.

Tsenga H.-H., Suc J.-G. and Liangc C. (2011), Synthesis of granular activated carbon/zero valent iron composites for simultaneous adsorption/dechlorination of trichloroethylene, *Journal of Hazardous Materials,* **192**, 500– 506.

Wang J., Han X., Ma H., Ji Y. and Bi L. (2011), Adsorptive removal of humic acid from aqueous solution on polyaniline/attapulgite composite, *Chemical Engineering Journal,* **173**, 171-177.

Wang X., Wu Z., Wang Y., Wang W., Wang X., Bu Y. and Zhao J. (2013), Adsorption–photodegradation of humic acid in water by using ZnO coupled TiO 2/bamboo charcoal under visible light irradiation, *Journal of Hazardous Materials,* **262**, 16-24.

Wu Y., Zhou S., Ye X., Zhao R. and Chen D. (2011), Oxidation and coagulation removal of humic acid using Fenton process, *Colloids and Surfaces A: Physicochemical and Engineering Aspects,* **379**, 151-156.

Yavich A.A., Lee K-H., Chen K-C., Pape L. and Masten S.J. (2004), Evaluation of biodegradability of NOM after ozonation, *Water Research,* **38**, 2839-2846.

Zhan X., Gao B., Yue Q., Wang Y. and Cao B. (2010), Coagulation behavior of polyferric chloride for removing NOM from surface water with low concentration of organic matter and its effect on chlorine decay model, *Separation and Purification Technology,* **75**, 61-68.

Zhang W., Gao H., He J., Yang P., Wang D., Ma T., Xia H. and Xu X. (2017), Removal of norfloxacin using coupled synthesized nanoscale zero-valent iron (nZVI) with H 2 O 2 system: Optimization of operating conditions and degradation pathway, *Separation and Purification Technology,* **172**, 158-167.

Zhang W.H., Quan X. and Zhang Z.Y. (2007), Catalytic reductive dechlorination of p-chlorophenol in water using Ni/Fe nanoscale particles, *J Environ Sci (China),* **19**, 362-366.